# CHAPTER 2

---

# ELECTRON GUN DESIGN STUDY FOR 42 GHZ, 200KW GYROTRON*

---

*Part of this work has been submitted for publication as:

**S. K. Sharma,** U. Singh, N. Kumar, N. Sahu, N. Shekhawat, D. Srivastava, M. K. Alaria, P. K. Jain and A. K. Sinha, "Electron beam misalignment study of MIG for 42 GHz, 200 kW Gyrotron", Communicated for Publication in Journal of Fusion Energy (Under revision).

## 2.1 Introduction

As discussed in the previous chapter, Chapter 1 of this thesis, that one of the most critical subassembly of the gyrotron is its electron gun which generates a helically gyrating electron beam for the interaction with the RF waves for the production of large RF power output from the device. The gyrating electron beam in a gyrotron is generated with the help of an electron gun assembly, which is popularly known as the 'magnetron injection gun' (MIG), so called as the shape of the gun structure is superficially similar to that of the interaction region of a traveling wave cylindrical magnetron [Goldenberg *et al*. (1973), Hermannsfelt (1979), Kartikeyan *et al*. (2004), Krivosheev *et al*. (2001), Singh *et al*. (2012), Tsimring (2007), Wenjie *et al*. (2009), Tsimring (2001)].

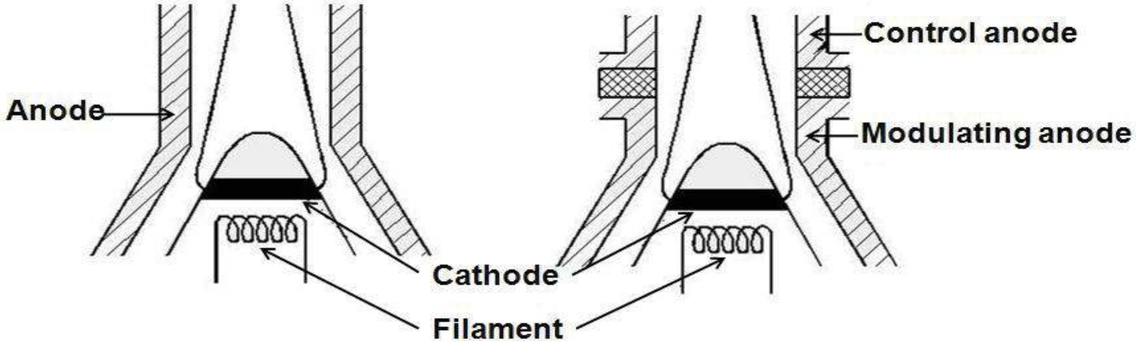

**Fig. 2.1:** Electron gun with diode and triode configuration [Singh (2012)].

MIGs are used as the electron gun for producing the helically gyrating electron beam which is operated in the temperature limited region and can be of two types, namely, diode-type and triode-type (Fig. 2.1). The diode-type MIG contains two electrodes, namely, cathode and anode (also called as control anode) and a high DC voltage is applied between them. Cathode basically acts as the source of electrons and thus kept at negative potential with respect to the other. In the triode-type MIG, three electrodes are present with the employment of an additional intermediate anode in between cathode and control anode. This intermediate anode is called modulating anode and kept at a higher potential with respect to the cathode potential but lower than the control anode potential. At the cathode surface, free electrons get liberated when the imparting energy applied due to potential between cathode and anode is higher than the work function of the cathode material. A typical value of magnetic field is applied at the cathode to put the emitted electron from the cathode under the influence of the DC magnetic field and thus causing the electrons to gyrate due to Lorentz force applied by the magnetic field on the electron beam. The gyrating beams advances further in the device towards the interaction structure under the influence of the electric field and the presence of the DC magnetic field and thus continue to gyrate. The radius of the orbital path of the electron beam, known as Larmor radius, progressively decreases as the magnetic field rises. Fig. 2.2 shows a typical gyrating electron beam obtained in a MIG.

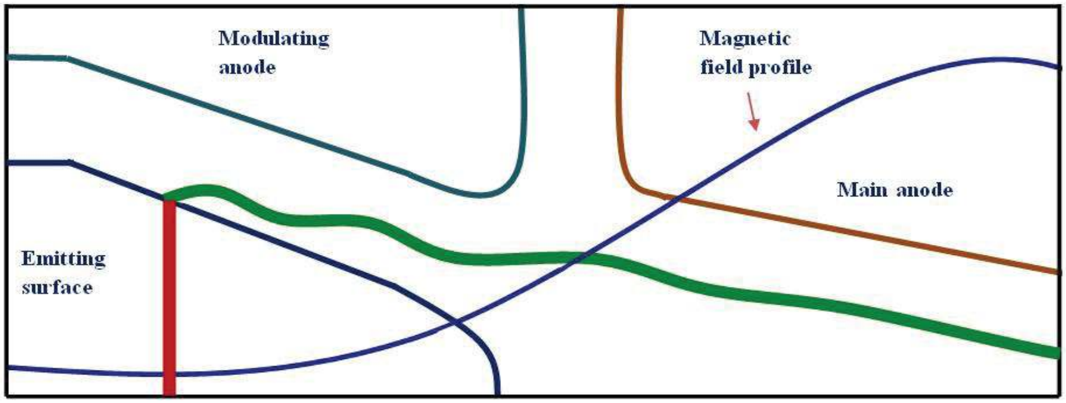

**Fig. 2.2:** Schematic view of a gyrotron electron gun showing the gyrating electron beam in green color [Singh (2012)]

The electron emitter, that is, cathode of the gyrotron MIG is typically a conical ring shaped structure, which facilitates in the formation of a hollow annular electron beam. The cathode used in the MIG is operated under the temperature-limited (TL) region rather than the space-charge-limited (SCL) region to minimize the electron beam velocity spread. The performance of the device depends to a large extent on the performance of the electron gun employed. The most common thermionic emitters also known as the cathodes have various options, such as, tungsten cathode, $LaB_6$ cathode, oxide-coated cathode, dispenser cathode, scandate cathode and thorium-based cathode, etc. The dispenser cathodes are presently widely used in the gyrotrons and also selected here for the gyrotrons under the present studies and thus to be explained slightly in detail here for the sake of completeness. The dispenser cathodes are made by compressing and sintering the tungsten powder into the shape of cylindrical billets from which a conical structure is fabricated. This porous tungsten matrix structure is impregnated with a mixture consisting of barium oxide (BaO), calcium oxide (CaO) and aluminum oxide ($Al_2O_3$). The composition of these three oxides is in a proportion 5:3:2 and is known as B-type dispenser cathode and in a proportion 4:1:1 is known as S-type dispenser cathode. In M-type disperser cathodes, an additional coating of Os or Re is used on the cathode emitting surface to further lower the work function of the cathode. The heating of cathode during its operation, causes the migration of barium towards the emitting surface where it lowers the work function. Although M-type cathodes coated with Os/Re have superior emission characteristics compared to B-type and S-type cathodes but they are more susceptible to gas poisoning. Lanthanum hexa-boride ($LaB_6$) cathode is also extensively used in the practical gyrotron which is an inorganic material, a boride of lanthanum. It has a melting point of ~2210°C and retains its strength at the high temperatures. It has a low work function of around 2.5eV and is stable in vacuum condition. They are also somewhat resistant to cathode poisoning.

In the present chapter, Chapter 2 of this thesis, the MIG is studied and designed through a systematic synthesis and analysis methodology. The synthesis is carried out with the help of the design trade-off equations [Baird *et al*. (1986)] and presented in Section 2.2. The synthesis gives the basic parameters of MIG electrodes related to cathode, anode, insulating ceramic and beam parameters related to beam voltage, beam current, etc. Then, the beam trajectory analysis is performed to achieve the shape of various electrodes and insulating ceramic (Section 2.3). The misalignment study of electron beam helps to study the performance of the electron gun in the practical assembly situation and thus is also carried out (Section 2.4).

## 2.2 Synthesis of the Magnetron Injection Electron Gun

The magnetron injection type electron gun for the gyrotron needs to be synthesized at first to get the initial design values of the several parameters. These are accomplished through the analytical expressions and the prior knowledge of the limiting values of the electron design parameters and are discussed as follow.

### 2.2.1 Analytical expressions of the electron gun design

Gyrotron operation requires a gyrating electron beam and, obviously, the electron beam quality also governs the performance of the device. The electron beam source assembly, that is, magnetron injection type electron gun produces a helical electron beam (HEB). The generation and propagation of helical electron beam in a MIG are performed under the influence of Lorentz force caused by the electric and magnetic fields. The propagation orbital path of the helical electron beam can be easily characterized by the electron beam parameters, namely, the electron cyclotron frequency or gyro-frequency ($\omega_c$), the beam radius ($R_b$) of the helical trajectory, the axial velocity of the electron beam ($v_z$), the transverse velocity of the electron beam ($v_\perp$) and the transverse-to-axial velocity ratio ($\alpha$), respectively. One can write the relations between the different velocities of the electron beam as [Tsimring (2007)]:

$$v_z = \frac{v}{\sqrt{1+\alpha^2}} \tag{2.1}$$

and

$$v_\perp = v_z \alpha \quad , \tag{2.2}$$

where $v$ is the net electron beam velocity. The transverse-to-axial velocity ratio ($\alpha$),which is the ratio of transverse velocity to axial velocity of the electron beam depends on the angle of the helical electron trajectory and should be >1 for the effective beam-wave interaction in the gyrotron device operation.

The helical electron beam formation is possible with the static electric and magnetic fields. Therefore, if we neglect initial velocities and dynamic instabilities, the spread of full electron velocities is equal to zero and thus one can write:

$$\Delta v^2 = \Delta({v_z}^2 + {v_\perp}^2) = 0\,. \tag{2.3}$$

Other characteristic parameter of the helical electron beam is the pitch $h_e$ of the helical trajectory. Taking into account the condition of the gyro-resonance $\omega \approx s\omega_c$ given by (1.3) and neglecting the Doppler effect, it can readily be written as [Tsimring (2007)]:

$$h_e = 2\pi \frac{r_\perp}{\alpha} \tag{2.4}$$

where $r_\perp$ is larmor radius, that is, radius of circular electron beam path.

For the design of MIG, some other basic parameters are required, such as, frequency of operation ($f_o$), RF output power ($P$), device efficiency ($\eta$), DC magnetic field at the RF cavity center ($B_o$), and beam radius at the cavity ($R_b$). The first two parameters, namely, frequency of operation and RF output power are specified by the user and are in the present case 42 GHz and 200 kW, respectively. The other two parameters, namely, DC magnetic field at cavity ($B_0$), and beam radius at cavity ($r_b$) are the parameters leading to the electron beam gyrating radius and electron beam launching radius at the centre of the RF interaction cavity and thus important parameters for the effective beam-wave interaction. The analytical expressions to estimate these parameters are discussed as follow.

When the electrons acquire a velocity perpendicular to the axial magnetic field, due to the the Lorentz force experienced by the electrons, starts moving in the circular motion with cyclotron frequency ( $\omega_c$ ) expressed through (1.1) and (1.3) as:

$$\omega_c = \frac{e\,B_o}{s\,m_o\,\gamma_0} \quad . \tag{2.5}$$

Here $s$ is the harmonic number and $\gamma_o$ is the relativistic mass factor. The DC magnetic field ( $B_o$ ) present at the RF interaction cavity region can be easily expressed from (2.5) as:

$$B_o(T) = \frac{f_o(GHz)\,\gamma_o}{28\,s} \quad . \tag{2.6}$$

The gyrotron under consideration is designed to operate in the fundamental mode (discussed in detail later in Chapter 4 of this thesis) and thus the harmonic number ($s$) = 1. Further, the relativistic mass factor can be written as:

$$\gamma_o = 1 + \frac{e\,V_o}{m_o\,c^2}\,, \tag{2.7}$$

where $V_0$ is the DC beam voltage and $c$ is the velocity of light in free space. For operation in $TE_{m\,n}$ mode, the electron beam radius ( $r_b$ ) can be given by [Kartikeyan *et al.* (2004)]:

$$r_b = \chi'_{m\pm i,s}\,\frac{r_o}{\chi'_{m,n}} = \frac{\lambda_o}{2\pi}\,\chi'_{m\pm i,s}\,. \tag{2.8}$$

Here, $i$ is the maxima ($i$ = 1, 2, 3, ...) of the RF field and $\chi'_{m,n}$ is the $m^{\text{th}}$ root of corresponding Bessel function ($TM_{m,n}$) or its derivative ($TE_{m,n}$).

The other parameters needed for the design MIG are related to the electron beam and the electron gun constituents. For example, beam voltage, beam current, velocity ratio, Larmor radius at the cathode, etc. are the parameters for the electron beam, while DC magnetic field at cathode, cathode radius, anode radius, anode voltage, etc. are the related parameters of the electron gun electrodes. The analytical formulae for the estimation of the initial values of these parameters are well established and briefed here, for the sake of ease and completeness [Baird *et al.* (1986)].

The magnetic compression ratio ($f_m$) gives estimation of magnetic fields at the cathode and defined as ratio of the magnetic fields at the cavity center ($B_o$) and cathode ($B_{zc}$), as:

$$f_m = \frac{B_o}{B_{z\,c}} \quad . \tag{2.9}$$

The electrons start moving in a helical path about a guiding center and this radius is small as compared to the electron beam radius of hollow gyrating electron beam. The radius of this path at cavity center, known as Larmor radius ($r_{lo}$) at the RF cavity is given as:

$$r_{lo} = \frac{\gamma_o}{B_o}\left(\frac{2\,m_o V_b}{e}\right)^{1/2} . \tag{2.10}$$

The electron beam guiding radius is the other parameter of the electron beam in the interaction region, which is decided by the launching position of the electron beam. The beam guiding radius ($r_g$) can be found with the help of beam radius and Larmor radius at the cavity as:

$$r_g = \sqrt{R_b^2 - r_{lo}^2} \quad . \tag{2.11}$$

Another normalized electron gun design parameter, namely, the gap factor ($D_f$) and the cylindricity factor ($\mu$) are defined as:

$$D_f = \frac{d_{ac}}{r_{lc}} \tag{2.12}$$

and

$$\mu = \left(\frac{1}{R_g^2 - 1}\right)^{1/2} \tag{2.13}$$

where $d_{ac}$ is the slant spacing between cathode and anode, $r_{lc}$ is the Larmor radius at cathode and $R_g$ is the ratio of beam guiding radius and Larmor radius at cavity and is called as the normalized guiding radius. The magnetic compression ratio ($f_m$) for small value of Larmor radius at cavity ($r_{l0}$) with respect to beam guiding radius ($r_b$) may also be defined as:

$$f_m = \left(\frac{\mu\, r_c}{r_{lo}}\right)^2 . \tag{2.14}$$

Cathode radius ( $r_c$ ) can be estimated from (2.11) and (2.14) under the condition for $r_g >> r_{lo}$ as:

$$r_c = (f_m)^{1/2}\, r_g \; . \tag{2.15}$$

The cathode and guiding radii are normalized with respect to the Larmor radius at interaction region ($r_{lo}$) and expressed these parameters as the normalized cathode radius ($R_c$) and the normalized guiding radius ($R_g$) and defined respectively as:

$$R_c = r_c / r_{lo} \, , \tag{2.16}$$

and

$$R_g = r_g / r_{lo} \, . \tag{2.17}$$

The other MIG design parameters, namely, the electric field ($E_c$) at cathode, the cathode-anode spacing factor ($d_f$), the slant length of the beam-emitting surface ($l_s$) and the modulating anode voltage ($V_a$) are expressed as [Baird *et al.* (1986)]:

$$E_c = \frac{V_a \cos\phi_c / r_c}{\ln(1 + D_f \mu)} \quad , \tag{2.18}$$

$$d_f = \frac{d_{ac} \cos\phi_c}{r_c \; \mu} , \tag{2.19}$$

$$l_s = \frac{I_o}{2\pi \, r_c \, J_c} \quad , \tag{2.20}$$

$$V_a = \frac{m_o c^2}{e} \frac{\ln\left(1 + D_f \mu\right)}{\ln\left(1 + 2\mu\right)} \left\{ \left[ 1 + \frac{4}{\mu^2} \left( \frac{1+\mu}{1+2\mu} \right)^2 \left( \frac{\left(\gamma_o^2 - 1\right)}{R_c^2 \cos^2\phi_c} \right) \left( \frac{\alpha^2}{\alpha^2 + 1} \right) \right]^{\frac{1}{2}} - 1 \right\} \quad . \tag{2.21}$$

Expression for the current ratio ($J_C / J_L$) is defined as the ratio between the cathode current density ($J_c$) and the space-charge-limited current density ($J_L$) can be expressed as [Baird *et al.* (1986)]:

$$\frac{J_C}{J_L} = \frac{I_o r_c (1 + D_f \; \mu) \beta^2}{(14.66 \times 10^{-6}) l_s \cos^2\phi_c (V_a)^{3/2}} \quad , \tag{2.22}$$

and

$$\beta = \exp\left( \frac{-q}{2} \right) \left[ q + \frac{1}{10} q^2 + \frac{5}{300} q^3 + ....... \right] \quad , \tag{2.23}$$

where

$$q = \ln(1 + D_f \; \mu) \, . \tag{2.24}$$

The estimations of various design parameters of MIG are obtained from the design trade-off equations (2.5)-(2.24) given by Baird *et al.* (1986) and can be tuned to estimate the initial design values under their limiting values.

### 2.2.2 Limiting values of the electron gun parameters

The design of magnetron injection electron gun needs several parameters for its design, as discussed above. Some of the parameters are fixed, such as, frequency of operation, output power, etc. as per requirement of the user. However, some of the parameters are achieved only through the analytical appreciations. Thus, some range or limits of these design parameters are certainly required for the ab-initio design. Based upon literature and experience, the limits of the values of these parameters are defined and presented in Table 2.1. Here, it is important to mention that the design criteria regarding to the cathode angle is taken as $\phi_c > 25°$ because, for a high current electron beam, the influence of the space charge effect on the velocity spread is an important factor. To reduce the space charge influence, $\phi_{eB}$ (angle between the emitter surface and the magnetic field lines) should be greater than 25°. In this case the laminar beam is formed and, therefore, the velocity spread growth with beam current is reduced [Tsimring (2001), Tsimring (2007)]. The criteria for another design parameter, that is, electric field breakdown ($E_b$) is also presented and this design parameter helps to estimate the distance between two electrodes of MIG for safe high voltage operation.

**Table 2.1:** Limit values of parameters in the MIG design

| Parameter | Limit value |
|---|---|
| Current ratio ( $J_C / J_L$ ) | < 0.2 |
| Cathode angle ( $\phi_c$ ) | > 25° |
| Cathode current density ( $J_C$ ) | 1 A/cm$^2$ to 2 A/cm$^2$ |
| Gap factor ( $D_f$ ) | > 3 |
| Electric field at cathode ( $E_c$ ) | 20 kV/cm to 60 kV/cm |
| Electron beam velocity spread ( $\delta\beta_\perp$ ) | < 5% |
| Electric field breakdown ( $E_b$ ) ( in vacuum) | < 5 kV/mm |
| Magnetic compression ratio ( $f_m$ ) | $10 < f_m < 30$ |
| Potential at modulating anode ( $V_a$ ) | < 50% of beam voltage |
| Relativistic factor ( $\gamma_o$ ) | 1.1 to 1.2 |
| Transverse-to-axial beam velocity ratio ( $\alpha$ ) | < 1.5 |

### 2.2.3 Synthesis of the electron gun

The synthesis of the gyrotron electron gun essentially requires the initial values of various parameters of electron beam, electrode as well as cathode. With the selections of the efficiency and the output RF power of the gyrotron, a simple method developed herewith is used to estimate the beam voltage and current. The beam voltage is selected through the estimation of the relativistic mass factor ($\gamma_o$) keeping its value less than1.15 which is the mean of the criteria value of relativistic mass factor given in Table 2.1. A number of values of $V_o$ are considered at different values of $\gamma_o$ starting from 1.15 and reducing it in steps using the well known expression (2.7) for $\gamma_o$ in terms of $V_o$, the charge of an electron ($e$) and the mass of an electron ($m_o$). The value of $V_o$ thus found is used to find beam current ($I_0$) from the beam power which, in turn, is known from the envisaged required device output power (here, 200 kW) combined with the device efficiency, the latter taken as ~30%. The approach discussed are used to find several possible combinations such as (i) $V_o = 70\text{kV}$, $I_o = 9.4\text{A}$, (ii) $V_o = 65\text{kV}$, $I_o = 10.2\text{A}$, and (iii) $V_o = 60\text{kV}$, $I_o = 11.0\text{ A}$ corresponding to $\gamma_o$=1.15, 1.13, and 1.10, respectively, with efficiency as 33% instead of 30% to keep design relaxation. However, here, the combination (ii) is chosen in order to keep a moderate relativistic factor and the beam current around 10A.

The minimum distance between the modulating and the control anodes is kept as such that there would be no high voltage breakdown. The cathode-anode (modulating) distance is estimated by dividing the maximum value of modulating anode voltage ($V_{a_{\max}}$) to the minimum value of the voltage breakdown limit ($V_{b_{\min}}$) in the vacuum. The operating mode is selected as the $TE_{0,3}$ mode with the second maximum of the transverse-plane field pattern of the cylindrical interaction cavity as the beam launching position for the fundamental beam-mode operation (see, Chapter 4) for the required power growth equal to 200 kW and beam-wave interaction is kept as fundamental for the higher efficiency. On the basis of above discussion, the input values for the synthesized parameters of MIG are found as beam voltage ($V_o$) = 65kV, beam current ($I_o$) = 10A, transverse-to-axial beam velocity ratio ($\alpha$) = 1.5, magnetic compression ratio ($f_m$) = 20 and cathode-anode distance ($d_{ac}$) = 7mm. Then, by using the design equations (2.5)- (2.24) and the design criteria mentioned in Table 2.1, a computer program "MIGSYN" has been indigenously developed in MATLAB. With the help of MIGSYN and the input values as discussed above, the synthesized values of various parameters of MIG have been obtained and presented in Table 2.2.

**Table 2.2:**Final values of MIG synthesized design parameters.

| MIG Parameter | Synthesized Value | Final Value |
|---|---|---|
| Frequency ( $f_o$ ) | 42GHz | 42GHz |
| Operating mode | $TE_{0,3}$ | $TE_{0,3}$ |
| Beam current ( $I_o$ ) | 10A | 10A |
| Beam radius ( $r_b$ ) | 6.06 mm | 6.06 mm |
| Beam voltage ( $V_o$ ) | 65 kV | 65 kV |
| Cathode angle ( $\phi_c$ ) | 25° | 28° |
| Cathode radius ( $r_c$ ) | 22.6mm | 22.55mm |
| Cathode-anode distance ( $d_{ac}$ ) | 7mm | 7mm |
| Modulating anode voltage ( $V_a$ ) | 32.5 kV | 29 kV |
| Magnetic compression ratio ( $f_m$ ) | 20 | 14.9 |
| Slant length of emitting surface ( $l_s$ ) | 6.4 mm | 7.0 mm |
| Magnetic field at interaction region ( $B_o$ ) | 1.65T | 1.61T |
| Transverse-to-axial beam velocity ratio ( $\alpha$ ) | 1.5 | 1.26 |

## 2.3 Gyrating Electron Beam Trajectory Analysis

The gyrating beam trajectory analysis provides information about the nature of beam gyration, propagation, launching, etc. Further, the beam trajectory analysis also yields the inner shape of the various electrodes for the effective propagation of the gyrating electron beam. The synthesized values of different parameters of the electron beam, cathode, anode, magnetic field, etc. are used to form an initial model for beam trajectory analysis from cathode to the RF cavity in a MIG. These synthesized values of the electron gun parameters are optimized through beam trajectory analysis which is performed with the help of a commercially available and widely used software EGUN developed by Herrmannsfeldt at the Stanford Linear Accelerator Center. EGUN code is a 2½ dimensional code in which the electrostatic and magnetostatic fields in two dimensions and particle trajectories in three dimensions are solved [Herrmannsfeldt (1979)]. The EGUN software is successfully used in various types of microwave tube covering both slowwave and fast-wave tubes for the analyses and designs of [Singh *et al* (2011), Singh *et al* (2012), Sharma *et al* (1999), Sharma *et al.* (2001), Sharma *et al.* (1999), Sharma *et al.* (2000), Sharma *et al.* (2002)]. The trajectory analyses have been performed for a range of values for various parameters. Fig. 2.3 shows the optimized design of MIG for 42 GHz, 200 kW gyrotron while Table 2.2 presents the optimized values of MIG. The other two important optimized parameters of MIG are also obtained from the trajectory analyses as maximum transverse velocity spread ($\delta\beta_{\perp\max}$) = 2.65 % and the distance between cathode and cavity centers = 330 mm. The sensitivity analyses of MIG performance with respect to all the MIG parameters, such as, magnetic field, cathode radius, cathode angle, beam voltage, beam current, modulating anode voltage, etc. are carried out to set the fabrication and performance tolerances. It is found that beam voltage = $65 \pm 1$ kV, the modulating anode voltage= $29 \pm 0.5$ kV, beam current = $10 \pm 2$ A, magnetic field at cathode = $1130 \pm 40$ gauss, cathode radius = $22.55 \pm 0.05$ kV, etc. can be easily tolerated without the effective deterioration of beam performance particularly from velocity ratio, velocity spread. beam launching radius, etc.

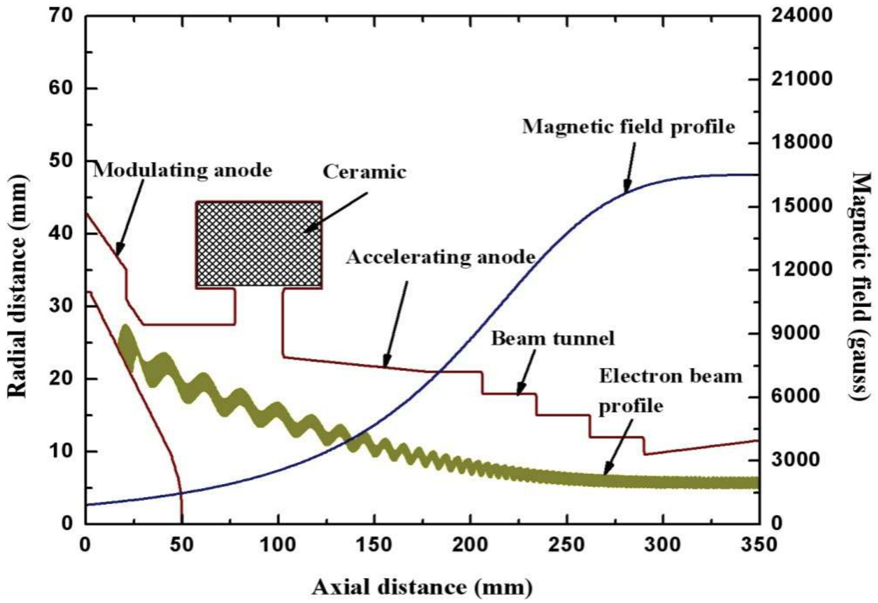

**Fig. 2.3:** The optimized design/ geometry of MIG for 200 kW, 42 GHz gyrotron ($V_o = 65$kV, $V_a = 29$kV, $I_o = 10$A, $B_o = 1.61$T/ 1.65T, $f_m = 14.9$ $B_{zc} = 0.108$T/ 0.11T).

## 2.4 Electron Beam Misalignment Study

The hollow annular gyrating electron beam in a gyrotron cavity cannot be placed concentrically with the system axis of the RF cavity and the system axis of magnetic field, in actual practice. This misalignment of electron beam axis from the system axis affects the gyrotron operation behavior. In the joining process during tube assembly, the piece parts position can be deviated from the designed values which can lead toward the degradation of beam quality parameters. The output RF power, power losses at the wall of the device and operating frequency performance of the device are thus affected with degradation of beam quality. In a triode type MIG, the position of cathode is sensitive to beam quality. Although the beam quality can be tuned with modulating anode voltage and cathode magnetic field, but to decide a general tolerance for the fabrication of MIG, the sensitivity studies of radial position of cathode, axial position of cathode, cathode magnetic field and cavity magnetic field are performed.

### 2.4.1 Study of the cathode position misalignment

The conical cathode is used as the electron emitter in the magnetron injection gun of the gyrotron. If the cathode is misaligned with respect to its position (axially and/or radially) then this affects the parameters, like, electron beam radius, electron launching position, electron velocity ratio, electron velocity spread, output power, operating mode, operating frequency, etc.

Figs. 2.4 and 2.5 show the possibilities in the misalignment of cathode in radial and axial direction from its original position. Figs. 2.6 and 2.7 show the effect of cathode misalignment on the transverse-to-axial velocity ratio and the maximum transverse velocity spread. The simulation results show that the cathode misalignment equal to ±0.50 mm in the radial and axial directions is tolerable with respect to the transverse-to-axial velocity ratio and the maximum transverse velocity spread, respectively.

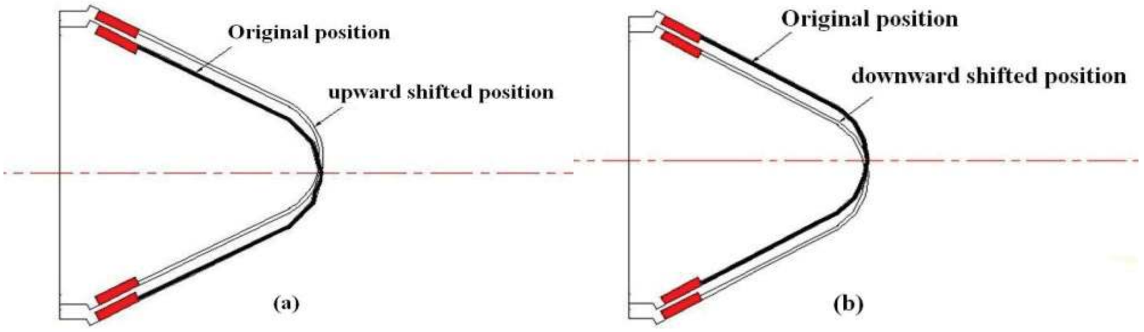

**Fig. 2.4:** Misalignment in radial (upward or downward) direction with its original position

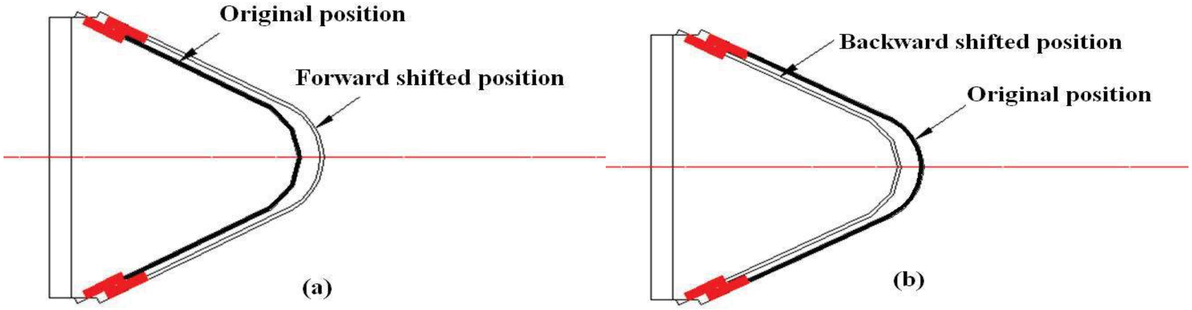

**Fig. 2.5:** Misalignment in axial (forward or backward) direction with its original position.

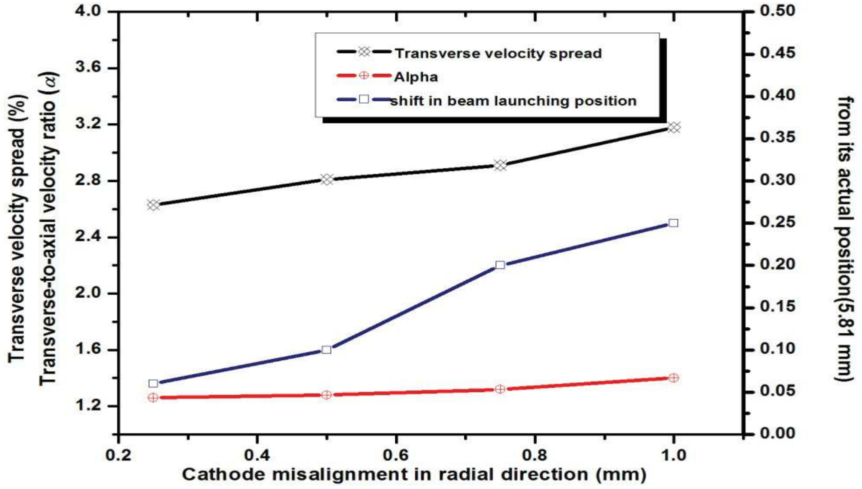

**Fig. 2.6:** Transverse to axial velocity ratio and maximum transverse velocity spread with radial misalignment of cathode

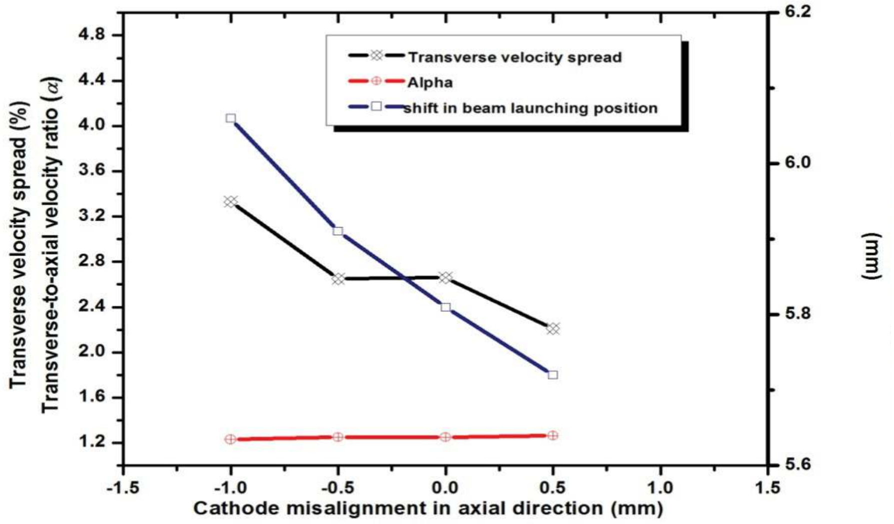

**Fig. 2.7:** Transverse-to-axial velocity ratio and maximum transverse velocity spread with axial misalignment of cathode

### 2.4.2 Study of the DC magnetic field misalignment

In the adiabatic flow of electron beam, the transverse velocity of the electron beam is inversely proportional to the cathode magnetic field. Figs. 2.8 and 2.9 show the effect of shifting of cathode magnetic field and cavity magnetic field on the various gyrotron electron source parameters such as the transverse velocity spread, electron beam velocity ratio and beam launching position in the cavity. It is clear from Figs. 2.8 and 2.9 that the electron beam radius is increased with increase in the cathode magnetic field. It can also be seen from this study that all the beam quality parameters are under desirable range ($\alpha > 1.1 < 1.5$, velocity spread < 5%) for the cathode magnet field shift from -8 gauss to 8 gauss. The cathode magnetic field can be controlled by varying the current of the cathode coil.

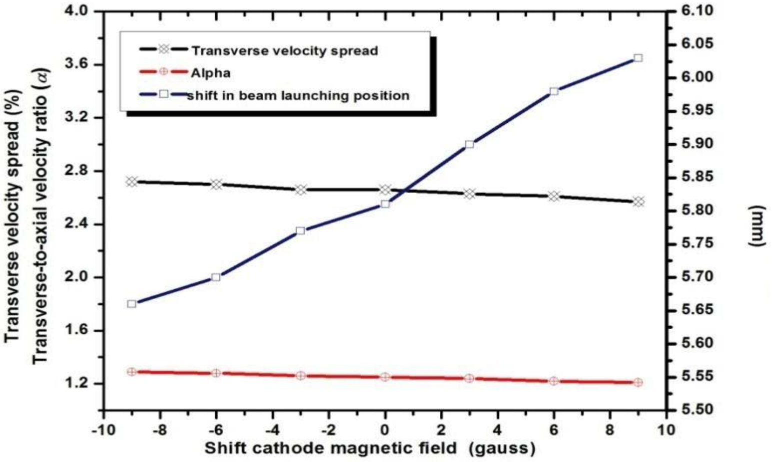

**Fig. 2.8:** Transverse to axial velocity ratio and maximum transverse velocity spread with cathode magnetic field shifting.

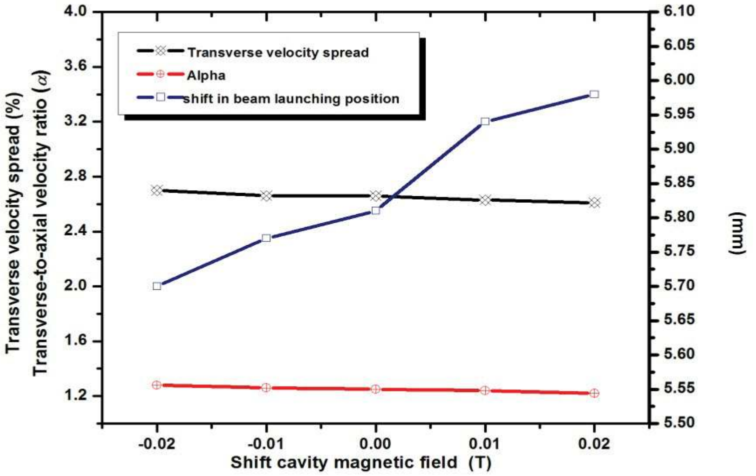

**Fig. 2.9:** Transverse to axial velocity ratio and maximum transverse velocity spread with cathode magnetic field shifting.

## 2.5 Measurement of the Cathode Misalignment

The misalignment of cathode position with respect to the facing modulating anode was carried out. For this purpose, at first, cathode-anode assembly was fabricated (Fig. 2.10). The measurement was made with the help of Nikkon microscope having least count 0.001 mm capability (Fig. 2.11). The gap between the lower part of cathode and the inner surface of modulating was measured at two positions in one straight line at various angular positions around the circumference. Some typical results are shown in Table 2.3 which clearly shows that the maximum misalignment in the axial gap is within the simulated to tolerable value of 0.5 mm.

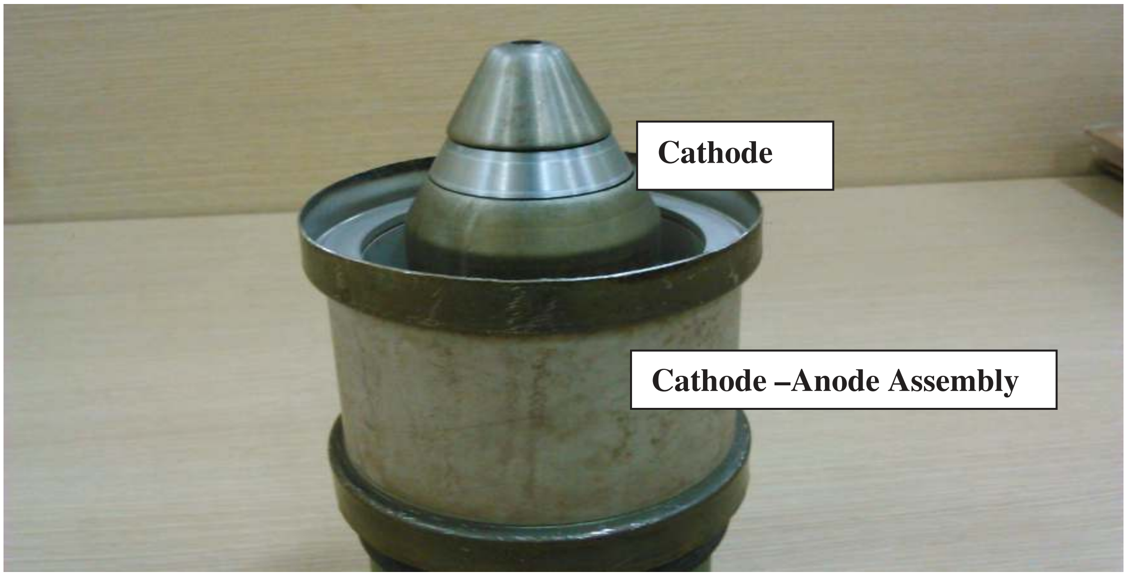

**Fig 2.10:** Cathode assembled with modulating anode

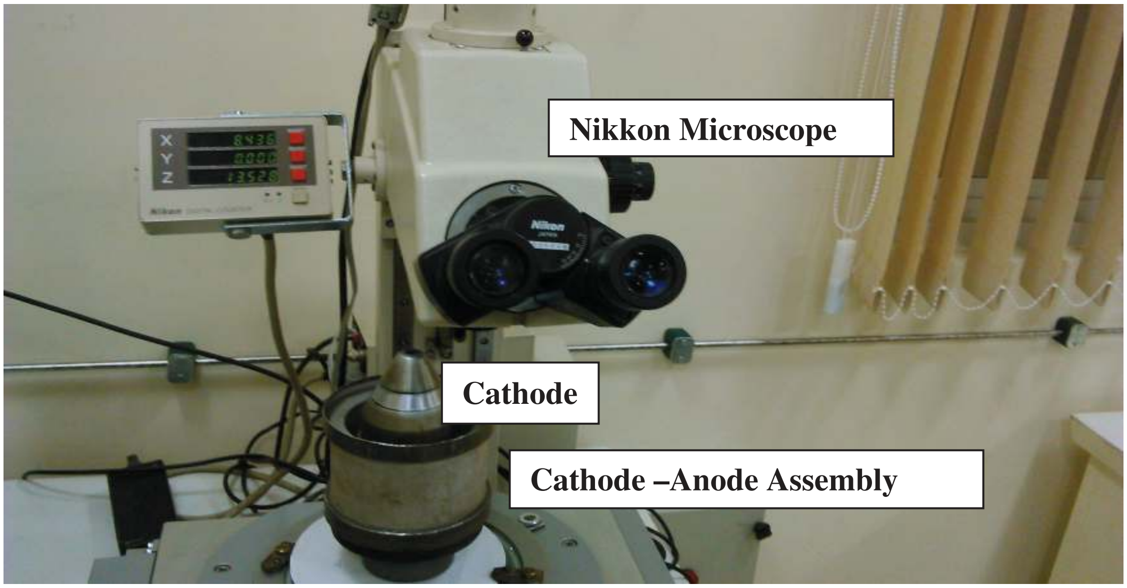

**Fig. 2.11:** Alignment measurement of cathode in cathode-anode assembly.

**Table 2.3:** Measurement data of cathode misalignment.

| **S. No.** | **Left Gap (mm)** | **Right gap (mm)** | **Cathode Misalignment (mm)** |
|---|---|---|---|
| 1 | 8.203 | 7.756 | 0.447 |
| 2 | 8.130 | 8.062 | 0.068 |
| 3 | 7.705 | 8.436 | 0.431 |
| 4 | 7.846 | 8.062 | 0.422 |

## 2.6 Extended Applicability of the 42GHz Gyrotron Electron Gun

The magnetron injection electron gun (MIG) is successfully designed here for a 42GHz, 200kW gyrotron and described in Sections 2.2 and 2.3 of this Chapter 2. The MIG is designed for the beam voltage = 65kV and beam current = 10A. It is of interest to explore the applicability of this 42GHz, 650kW gyrotron electron gun for its use in another usable gyrotron of some other frequency, such as, 28GHz gyrotron used for material processing and also for ECRH application. In this direction, an attempt has been made to see the extended applicability of the 42GHz MIG with the same dimensional geometry so that the MIG can be used for another frequency just by changing the flexible parameters outside the MIG.

**Table 2.4:** Basic specifications of 28GHz, 100kW gyrotron.

| **Parameter** | **Value** |
|---|---|
| **Frequency** | **28 GHz** |
| Operating mode | $TE_{3,2}$ |
| Beam launching position | 5.21 mm |
| Output power (*P*) | 100kW |
| Beam voltage ($V_b$) | 65 kV |
| Beam current ($I_b$) | 10 A |

In the design and operation of a MIG, the launching of electron beam in the interaction cavity is an important parameter. In the Section 2.3, the results of electron beam analysis for 42 GHz, 200kV gyrotron MIG are discussed. A new approach is followed here to use the same MIG for 28GHz, 100kW gyrotron MIG with different launching position equal to 5.21mm of the electron beam in the interaction cavity with the different operating mode $TE_{3,2}$. The basic specifications of new frequency MIG are given in Table 2.4. Here the tuning of electron beam launching position has been carried out by using the extra magnet coil at the cathode. As mentioned above, the dimensions of the cathode as well as the anodes are kept the same as for

42GHz, 200kW gyrotron mentioned in the last column as the final value of Table 2.2. It is of interest to mention that the same MIG can be easily employed for the generation of 100kW output power with the operating mode $TE_{3,2}$ as discussed in Section 4.6 of Chapter 4.

**Table 2.5:** Optimized parameters of MIG for 28GHz, 100kW gyrotron.

| **Parameter** | **Value** |
|---|---|
| Magnetic compression ratio ( $f_m$ ) | 14.8 |
| Cathode current density ( $J_c$ ) | 1 A/cm$^2$ |
| Modulating anode voltage ( $V_a$ ) | 15 kV |
| Beam radius ( $r_b$ ) | 5.3 mm |
| Maximum transverse velocity spread ( $\delta\beta_{\perp\max}$ ) | 4 % |
| Transverse-to-axial beam velocity ratio ( $\alpha$ ) | 1.3 |
| Magnetic field at interaction region ($B_o$) | 1.05 T |

After a lot of iterations, the MIG electrical design is optimized for 28 GHz, 100 kW gyrotron with the help of EGUN code. The final optimized parameters are given in Table 2.5. The electron beam trajectory with MIG geometry and magnetic field is shown in Fig. 2.12. The simulation of electron beam trajectory analysis very clearly states that MIG of 42GHz, 200kW MIG can be easily used for 28GHz, 100kW gyrotron.

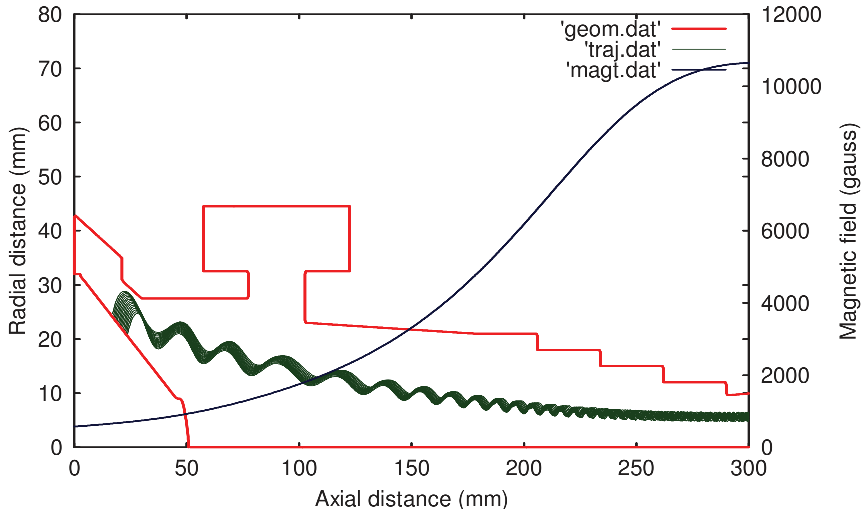

**Fig. 2.12:** MIG with electrode geometry, beam profile and magnetic field profile optimized by using EGUN code for 100kW, 28GHz gyrotron.

## 2.7 Conclusion

Gyrotron electron gun, MIG which produces hollow annular helically gyrating electron beam is the most complex assembly in the gyrotron. It consists of many metal and ceramic piece-parts as well as the fragile cathode-heater sub-assembly. An in-house design methodology has been developed with the proper combination of the in-house and commercial codes so that all the steps, such as, synthesis, beam trajectory analysis, etc. have been carried out. The developed design methodology has been successfully applied for the optimization and design of all the relevant parameters of electron beam and electrodes of the MIG including the cathode. The synthesis based upon the available analytical expressions is used for the estimations of the initial values of all the design parameters. Then, with the help of electron beam trajectory analysis, the design of MIG is optimized and the cathode as well as the anode dimensions as well as electron beam parameters such as magnetic field = 1.61T, beam voltage = 65kV, beam current = 10A, velocity ratio = 1.26, etc. are finalized. The misalignment studies of the cathode are also carried out to see the performance tolerance. It is interest to mention that the extended applicability of 42GHz MIG has been explored. It is found 42GHz MIG can be easily employed at another gyrotron frequency, that is, 28GHz for 100kW gyrotron with the changed interaction cavity parameters.

The studies carried out in the present chapter will be extended further and reported in the subsequent chapters of the thesis for the design and development of other assemblies of the gyrotron. In the next chapter, Chapter 3, the development of the cathode heater subassembly for the 42GHz, 200kW will be described.